9. Yakovlev, P. I. & Lecours, A. in *Regional Development of the Brain in Early Life* (ed. Minkowski, A.) 3–70 (Blackwell, Oxford, 1967).
10. Takeuchi, A. H. & Hulse, S. H. Absolute pitch. *Psychol. Bull.* **113,** 345–361 (1993).
11. Barnea, A., Granot, R. & Pratt, H. Absolute pitch-electrophysiological evidence. *Int. J. Psychophysiol.* **16,** 29–38 (1994).
12. Benguerel, A. P. & Westdal, C. Absolute pitch and the perception of sequential music intervals. *Music Percept.* **9,** 105–120 (1991).
13. Williamson, S. J. & Kaufman, L. in *Auditory Evoked Magnetic Fields and Electric Potentials* (eds Grandori, F., Hoke, M. & Romani, G. L.) 1–39 (Karger, Basel, 1990).
14. Kaas, J. H., Merzenich, M. M. & Killackey, H. P. The reorganization of somatosensory cortex following peripheral nerve damage in adult and developing mammals. *Annu. Rev. Neurosci.* **6,** 325–356 (1983).

Acknowledgements. We thank our subjects for their cooperation, K. Berning for assistance and A. Wollbrink for engineering. This research was supported by grants from the Deutsche Forschungsgemeinschaft and NATO.

Correspondence and requests for materials should be addressed to C.P. (e-mail: pantev@uni-muenster.de).

Dynamic cortical activity in the human brain reveals motor equivalence

J. A. S. Kelso*, A. Fuchs*, R. Lancaster*, T. Holroyd*, D. Cheyne† & H. Weinberg†

** Program in Complex Systems and Brain Sciences, Center for Complex Systems, Florida Atlantic University, Boca Raton, Florida 33431-0991, USA*
† Brain Behavior Laboratory, Discovery Park, Simon Fraser University, Burnaby, British Columbia V5A 1S6, Canada

That animals and humans can accomplish the same goal using different effectors and different goals using the same effectors attests to the remarkable flexibility of the central nervous system. This phenomenon has been termed 'motor equivalence'[1,2], an example being the writing of a name with a pencil held between the toes or teeth. The idea of motor equivalence has reappeared because single-cell studies in monkeys have shown that parameters of voluntary movement (such as direction) may be specified in the brain, relegating muscle activation to spinal interneuronal systems[3,4]. Using a novel experimental paradigm[5] and a full-head SQUID (for superconducting quantum interference device) array to record magnetic fields corresponding to ongoing brain activity, we demonstrate: (1), a robust relationship between time-dependent activity in sensorimotor cortex and movement velocity, independent of explicit task requirements; and (2) neural activations that are specific to task demands alone. It appears, therefore, that signatures of motor equivalence in humans may be found in dynamic patterns of cortical activity.

The first experiment required human volunteers to flex or extend the preferred index finger either on the beat of a metronome or between metronome beats, the frequency of which was fixed at 1 Hz (see Methods). Notice that these experimental conditions may be grouped either according to the kinematics of motion (flexion versus extension movements and their derivatives) or according to the coordination task (synchronization or syncopation). Figure 1 shows the relative phase between stimuli and movement peaks across cycles for all four conditions. As requested, the peak of the movement is synchronized closely to the stimulus in the flexion-on-the-beat and extension-on-the-beat conditions. Likewise, subjects are able to place a movement between stimuli in the flexion-off-the-beat and extension-off-the-beat, syncopation conditions. Also shown are histograms that measure task success. In general, the distributions for the syncopation conditions are broader than those for synchronization, indicating performance is more variable. Subjects had more difficulty syncopating than synchronizing, which conforms to everyday experience and behavioural evidence[5].

Brain activity was recorded continuously during these tasks, using a 64-channel magnetometer sampled at 250 Hz. All the magnetic fields generated by the brain arise from the flow of electrical current, which is mainly ionic and originates in the dendrites and cell bodies of cortical neurons[6]. Figure 2 gives an example of the field pattern shown on a model head (Fig. 2a) and the same pattern shown in polar projection on the plane (Fig. 2b). The dominant field over the sensorimotor area of the left hemisphere is expected for right-handed movements. How is this evolving brain activity related to the behaviour produced? Figure 3a shows cortical activity patterns averaged across subjects for each task sampled at various time points (red line) throughout the movement. The average amplitude profile of the movement is also shown (green line). To ease viewing across conditions, the movement profiles are all plotted in the same positive-going direction. Notice the strong dipolar field in the sensorimotor area of the left hemisphere during the first part of the movement, regardless of whether it involves flexion or extension. Notice also that the field reverses just after the peak movement (column 5) and then becomes much weaker and more distributed. Figure 3b plots the time series of the average brain activity obtained from single sensors for the flexion-on (the beat) condition. On the lower left is plotted the movement profile and its derivative, velocity: particularly on the left side of the array, brain activity and movement velocity are nearly superimposed, as confirmed by correlation analysis. The cross-correlation between movement velocity and time-varying brain signal is almost 1 (or −1) in the yellow area of Fig. 3b, corresponding precisely to maxima and minima of the field.

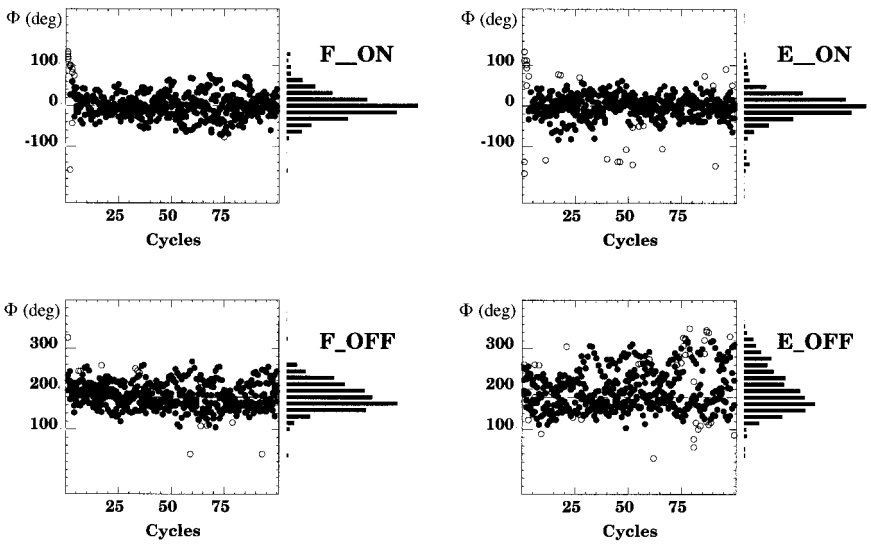

Figure 1 Relative phase across cycles for all conditions (top row, synchronization; bottom row, syncopation) and all subjects, a total of ~500 observations per condition. Solid circles indicate cycles within a ±60 degree range of the average phase for single subjects. Open circles are outside this range and were rejected from further analysis.

Elsewhere the correlation is much weaker and, in certain anterior and posterior regions, practically zero. This strong correlation between movement velocity and the time course of activity in left sensorimotor cortex is found in all four experimental conditions.

Decomposition of the brain's magnetic field into components corresponding to localized current sources is an ill-posed problem. Nevertheless, the spatial patterns of cortical activity shown in Fig. 3a are well localized and mostly stationary during particular phases of the task. We decomposed the brain signals into spatial patterns and time-varying amplitudes using two methods. The first, known as Karhunen–Loève (K–L) decomposition, or principal components analysis[7], calculates the eigenvectors of the covariance matrix between sensors x and y as an orthogonal basis. Tangential currents naturally produce spatial correlations (the field entering the scalp at one location and leaving at another; Figs 2, 3), and the resulting principal components may capture this dipolar structure. The

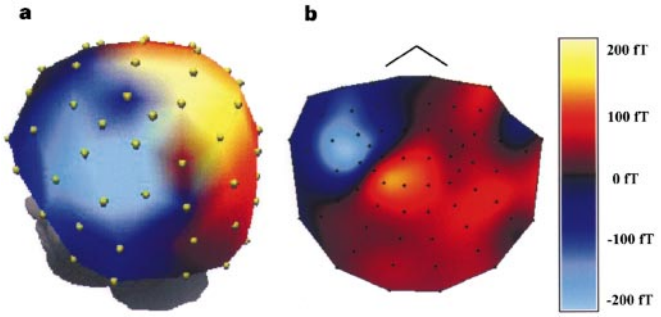

Figure 2 Neuromagnetic activity of the human brain. **a**, Sensor locations displayed on the subject's head, and **b**, corresponding polar projection. Blue indicates sites where the magnetic field is entering the head, and red-yellow indicates sites where the field is leaving the head. The field amplitude is in units of femtoTesla.

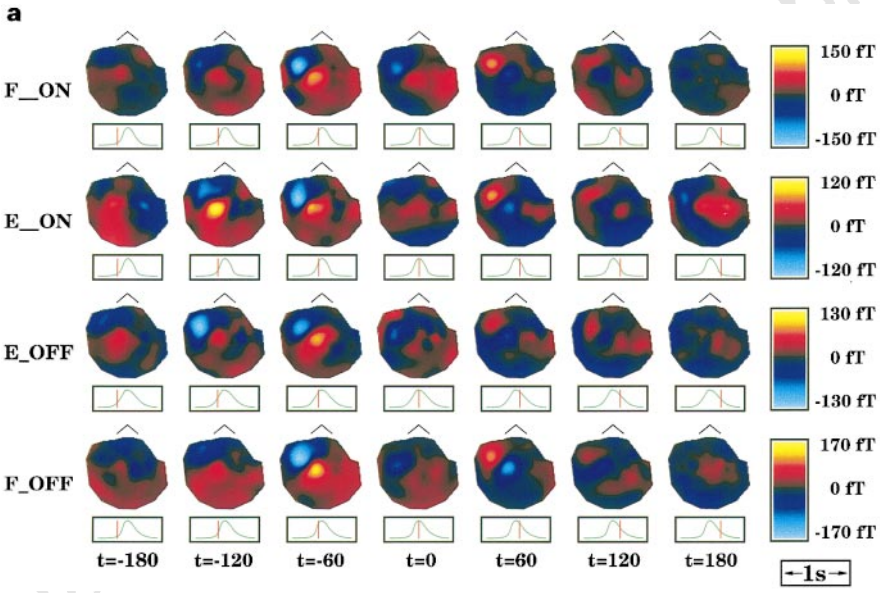

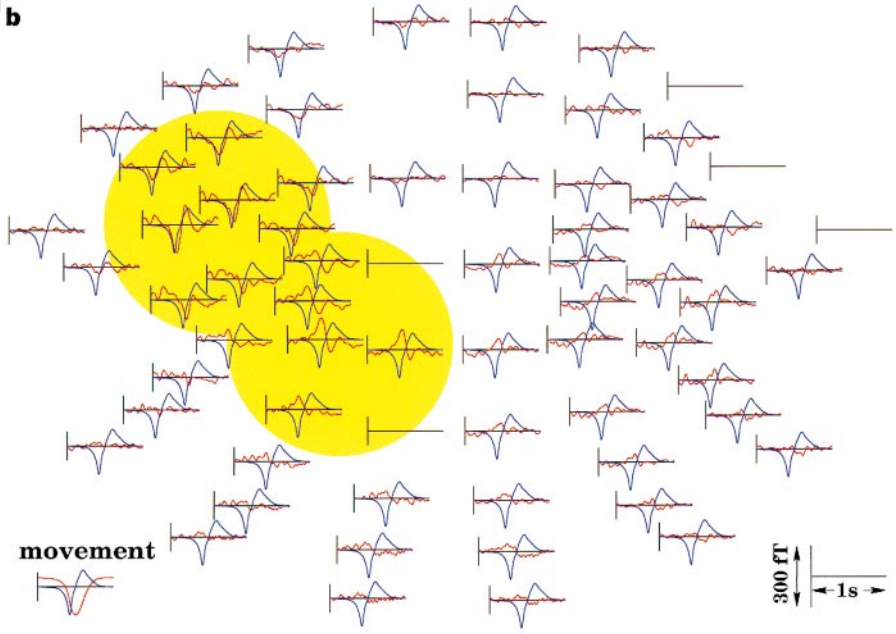

Figure 3 Cortical activity patterns for each experimental condition. **a**, Data are averaged across cycles and subjects at time points t (ms). Time point $t = 0$ is the peak movement amplitude. The green curve in the box shown below each pattern is the average amplitude profile for each condition. The red line indicates the time at which brain activity is sampled during the movement cycle. Each condition is scaled separately to highlight the peak fields. In general, the activity for flexion conditions has a slightly higher amplitude range than the extension conditions. **b**, Time series of averaged brain activity (red) across cycles and subjects for the flexion-on-the-beat condition. Overlaid (blue) is the movement velocity. In the centres of the yellow circles, the correlation between brain activity and movement velocity is close to ±1.

group averages shown in Fig. 4a indicate that the first spatial mode captures about 60% of the variance in the brain signals (the eigenvalue for each condition is given in the boxes). Because the top spatial mode, like the underlying neural generators, is under no orthogonality constraint, it is identical to the dominating spatial pattern of brain activity observed experimentally. Figure 4a shows that its time-dependent amplitude tracks the velocity profile extremely well, especially for the initial velocity peak associated with the active phase of the coordination task (see Methods). The second velocity peak constitutes the less active phase of the task, and the

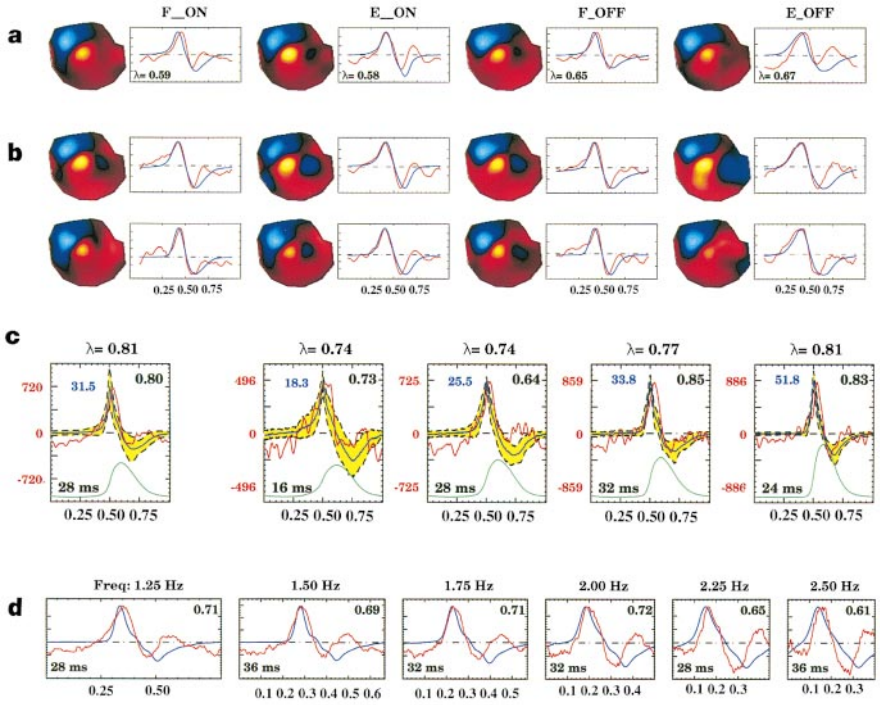

Figure 4 Relationship between cortical activity and movement velocity. **a**, The first spatial mode of a Karhunen–Loève decomposition and its time-dependent amplitude (red) averaged across subjects. Eigenvalues in the lower left corner of each box indicate how much of the variance of the entire signal is contained in a given mode. Movement velocity for each condition is shown in blue. **b**, The spatial pattern that best fits the time series of the movement velocity for the group (first row) and a single subject (second row) for all conditions. **c**, Scaling between brain activity (red) and movement velocity (blue/grey). Left box, average data for all conditions for the subject shown in **b**. Remaining boxes, data sorted in bins according to different peak velocities (blue numbers), which increase from left to right (standard deviation in yellow, bounded by dashed lines). Amplitude profiles shown in green are on a common scale. Black numbers indicate the eigenvalues (above each box), correlation values between brain activity and velocity profile (top right) and corresponding time lags in ms (bottom left). **d**, Effect of different movement rates. The smaller boxes as one moves from left to right reflect the number of points sampled in a given cycle, which decreases with movement rate.

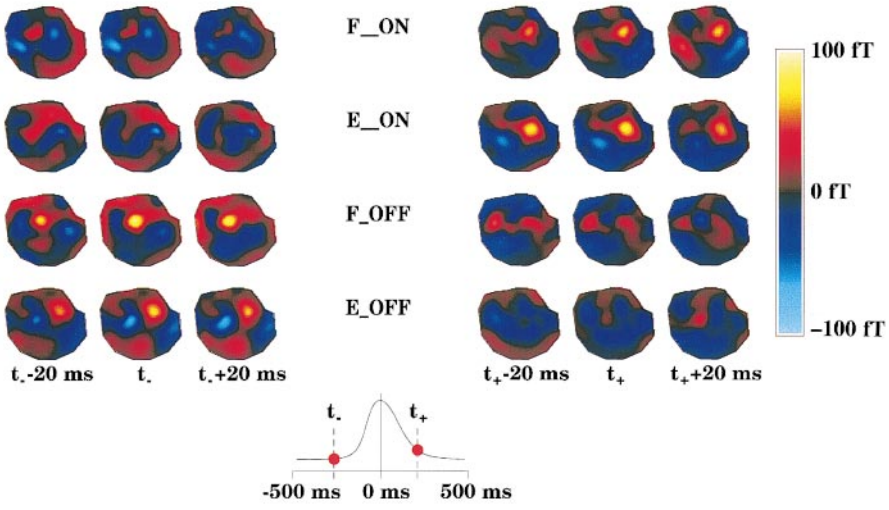

Figure 5 Brain activity fields for the four conditions in the first experiment, flexion and extension movements at 1 Hz, after the dominant spatial pattern (shown in Fig. 4b) was removed from the data set. The residual patterns sampled before the peak movement (left columns) indicate strong similarities across syncopation task conditions but large differences between synchronization and syncopation task conditions. Likewise, the residual patterns sampled after the peak movement (right columns) are similar across synchronization conditions, but different between syncopation and synchronization. The curve at the bottom represents the average amplitude profile for all conditions. Red circles indicate the time points around which brain activity was sampled. $\mathbf{t}_-$ and $\mathbf{t}_+$, Peak field amplitudes for syncopation and synchronization, respectively.

match to the brain signal is weaker. These results are striking because the K-L decomposition simply minimizes the mean-square error without regard to the movement at all. A second method calculates the spatial patterns that best fit the movement and its derivatives[8]. The results of this procedure are shown in Fig. 4b for the group (first row) and a single subject (second row). Once again, the largest mode corresponds to movement-related brain activity (see also Fig. 3a), specifically the velocity of finger flexion or extension.

Two questions arise from these results. First, is the strong relationship between average movement velocity and the time course of cortical activity a coincidence, or is it maintained across changes in the velocity profile? In particular, is this relationship consistent across different peak velocities (with the same length time course) and is it consistent across different movement rates (similar peak velocity, but shorter time course)? Second, what is the influence of the task alone on patterns of brain activation? To answer the first question, we used two approaches. First, we sorted the existing data from all four original experimental conditions into sets representing different peak velocity ranges, from slowest to fastest. The data from four different peak velocity ranges for a representative subject are shown in Fig. 4c. The brain signal (again the time-dependent amplitude of the top K–L spatial mode) is plotted (red) along with the velocity profiles (blue/grey) for the overall data (left box) and four non-overlapping bins, in which velocity increases from left to right. The steepness of the displacement profile (green) reflects the derivative (actual values in blue). Notice that each graph in Fig. 4c is scaled individually, highlighting the correspondence between brain signal and velocity profile. The degree of covariance, given by the correlation value on the top right of each box, is high.

Next, we asked the same subjects to perform the two basic syncopation tasks at six different movement rates (see Methods). Beginning either in the flexion- or extension-off-the-beat conditions, subjects were instructed to syncopate with the metronome, as its rate was increased in small steps of 0.25 Hz, every 10 cycles. Transitions from syncopation to synchronization occur spontaneously in both brain activity and behaviour as movement rate is increased beyond a critical value[9], but the relationship between velocity and cortical activity has not been examined before to our knowledge. The results were unequivocal across subjects, initial conditions and movement rates. Figure 4d shows a representative example for the flexion-off condition. The same basic dipolar-like spatial pattern was observed at all movement rates. For ease of viewing, the velocity profile (blue) is superimposed on the brain signal (here the best-fit spatial pattern, as in Fig. 4b, though the results for the top K–L mode are nearly identical). The value of the correlation function at the time lag between the first velocity peak and the brain signal is also reported (top right). Given the predictive, rhythmical nature of the task and the probable contribution of reafferent activity from the muscles to sensorimotor cortex[10–12], it is unsurprising that the peak movement velocity leads the cortical activity by a small amount (lower left corner of Fig. 4c and d). Yet the similarity in the neural and velocity profiles again is striking, especially in the initial active phase of voluntary movement.

To answer the second question, about task-specific brain activity, we removed the dominant velocity-related spatial pattern from the recorded brain signals. These residual brain patterns are shown in Fig. 5. Notice that the time course of brain activation now is very different for synchronization (top rows) and syncopation (bottom rows) tasks. Before the peak movement (left columns), the brain patterns for syncopation are similar to each other but different from the corresponding brain activity patterns for synchronization. Likewise, after the peak movement (right columns), synchronization conditions are nearly identical and very different from their syncopation counterparts. Any differences attributable to movement direction (for example, flexion-on and extension-off are kinematically similar) are far outweighed by differences due to the task. Thus, although their detailed physiological interpretation awaits clarification, the patterns of brain activation distinguishing the two tasks are compelling and seem to reflect higher-order task planning.

Finding a coherent neural signal that is specifically related to behaviour in such a complex system as the human brain is a challenge. Although obtained in different experimental circumstances, the discovery of a direct and robust relation between the time course of cortical activity and the movement derivative across a broad range of initial conditions, peak velocities and movement rates fits single-cell studies in monkeys that suggest that speed (in addition to direction[13,14]) is represented in the discharge rate of motor cortical cells[15]. Moreover, our findings help resolve a long-standing question in psychophysical studies of human sensorimotor coordination[16,17,18], how the brain coordinates actions in time with external events. It does so by generating a neural activity pattern that significantly mirrors the movement derivative or velocity. At the same time, dynamic patterns of cortical activity are task specific. □

Methods

Task. In the first experiment, subjects ($n = 5$) were instructed to time the peak of their finger movements (synchronize or syncopate) to a visual metronome, which was a computer-controlled light-emitting diode (LED) located in the centre of the visual field, 2 m from the subject. This stimulus was delivered for 100 cycles at a frequency of 1 Hz. For each subject, we randomized the order of the four experimental conditions: flexion on the beat, extension on the beat, flexion off the beat and extension off the beat. A pair of small inflated plastic pillows connected to pressure sensors by plastic tubing was positioned so that the subject's preferred (right) index finger could slide between them. Small-amplitude, almost isometric flexion or extension movements about the metacarpophalangeal joint in the transverse plane increased the pressure in the pillow in the 'active' phase of the task. The passive action of the pillow helped return the finger to its starting position. All motions were transduced by pressure sensors into voltages. The locations of the movement peaks were calculated as the corresponding zero crossings in the derivative of the signal. From these movement peaks stimulus onsets, the relative phase between stimulus and response was calculated on every cycle. In a follow-up experiment that examined the effect of movement rate, the same subjects performed the two syncopation conditions at different metronome frequencies. Beginning in either flexion- or extension-off-the-beat at 1.25 Hz, the stimulus frequency was increased every 10 cycles in steps of 0.25 Hz up to 2.5 Hz. Each subject performed 40 runs in each of the two conditions, a total of 4,800 cycles of movement per subject.

Neuromagnetic measurements. The metronome and pressure-sensor voltages from the response pillows were digitized, along with 64 channels of magnetic field data. The SQUID sensor array (CTF Systems) consisted of 64 first-order gradiometers uniformly distributed over both hemispheres. Each gradiometer had a baseline of 5 cm and a coil diameter of 2 cm. Third gradient response was calculated using a system of reference coils. The sampling rate for all signals was 250 Hz with a 40 Hz low-pass filter and notch filters at 60, 120 and 180 Hz.

Analysis. Two different but related methods of spatiotemporal analysis were applied to the dataset. One was Karhunen–Loève decomposition or principal components analysis, in which the covariance matrix of the time series for single sensors is calculated and diagonalized. The eigenvectors of this matrix represent spatial patterns that are used as basis vectors for the decomposition of the signal. How much power these single patterns contribute to the entire signal is given by the eigenvalue corresponding to the pattern. In many cases, only a few of these modes (here two or three) are needed to capture 80–90% of the variance. A time series (Fig. 4) for each of the spatial patterns is calculated by projecting the signal onto the basis vectors. This method simply creates an orthogonal basis with the axes pointing in the direction of maximal variance (for the higher modes, under the orthogonality constraint), although the dominating mode is related closely to the movement velocity (Fig. 4a). Therefore, we applied a second method that actually takes the velocity of movement into account, calculating a spatial pattern that best fits a given time series. The aim of this method is to find a spatial pattern that yields a minimum

mean-square error if multiplied with a given time series (say, movement velocity) and subtracted from the original signal at each time point. This pattern is given by $P_i = \langle v(t)H_i(t)\rangle/\langle v^2(t)\rangle$, where P_i is the pattern at the location of the ith sensor, $H_i(t)$ is the activity in this sensor, $v(t)$ is the time series (here, movement velocity) and $\langle\ldots\rangle$ denotes a temporal average.

Received 16 September 1997; accepted 30 January 1998.

1. Lashley, K. S. Basic neural mechanisms in behavior. *Psychol. Rev.* **37,** 1–24 (1930).
2. Hebb, D. O. *The Organization of Behavior: A Neuropsychological Theory* (Wiley, New York, 1949).
3. Bizzi, E., Mussa-Ivaldi, F. & Giszter, S. Computations underlying the execution of movement: a biological perspective. *Science* **253,** 287–291 (1991).
4. Georgopoulos, A. P. Neural networks and motor control. *Neuroscientist* **3,** 52–60 (1997).
5. Kelso, J. A. S., DelColle, J. D. & Schöner, G. in *Attention and Performance XIII* (ed. Jeannerod, M.) 139–169 (Erlbaum, Hillsdale, New Jersey, 1990).
6. Romani, G. L. in *Advances in Biomagnetism* (eds Williamson, S. J., Hoke, M., Stroink, G. & Kotani, M.) 33–46 (Plenum, New York, 1989).
7. Fuchs, A., Kelso, J. A. S. & Haken, H. Phase transitions in the human brain: spatial mode dynamics. *Int. J. Bifurc. Chaos* **2,** 917–939 (1992).
8. Uhl, C., Friedrich, R. & Haken, H. Analysis of spatiotemporal signals of complex systems. *Phys. Rev. E* **51,** 3890–3900 (1995).
9. Kelso, J. A. S. *et al.* A phase transition in human brain and behavior. *Phys. Lett. A* **169,** 134–144 (1992).
10. Cheyne, D. & Weinberg, H. Neuromagnetic fields accompanying unilateral finger movements: pre-movement and movement-evoked fields. *Exp. Brain Res.* **78,** 604–612 (1989).
11. Kristeva, R., Cheyne, D. & Deecke, L. Neuromagnetic fields accompanying unilateral and bilateral voluntary movements: topography and analysis of cortical sources. *Electroencephalogr. Clin. Neurophysiol.* **81,** 284–298 (1991).
12. Wiesendanger, M. & Miles, T. S. Ascending pathway of low-threshold muscle afferents to the cerebral cortex and its possible role in motor control. *Physiol. Rev.* **62,** 1234–1270 (1982).
13. Georgopoulos, A. P., Kalaska, J. F., Caminiti, R. & Massey, J. T. On the relations between the direction of two-dimensional arm movements and cell discharge in primate motor cortex. *J. Neurosci.* **2,** 1527–1537 (1982).
14. Schwartz, A. B., Kettner, R. E. & Georgopoulos, A. P. Primate motor cortex and free arm movements to visual targets in three dimensional space. I. Relations between cell discharge and direction of movement. *J. Neurosci.* **8,** 2913–2927 (1988).
15. Moran, D. W. & Schwartz, A. B. Motor cortical representation of speed and direction during reaching. *J. Neurophysiol.* (in the press).
16. Bartlett, N. R. & Bartlett, S. C. Synchronization of a motor response with an anticipated sensory event. *Psychol. Rev.* **66,** 203–218 (1959).
17. Wing, A. M. & Kristofferson, A. B. The timing of interresponse intervals. *Percept. Psychophys.* **13,** 455–460 (1973).
18. Dunlap, K. Reactions to rhythmic stimuli. *Psychol. Rev.* **17,** 399–416 (1910).

Acknowledgements. This research was supported by NIMH (U.S.A.), NSERC (Canada) and the Human Frontier Sciences Program. We thank M. Burbank and J. Vrba for the use of facilities at Port Coquitlam, British Columbia.

Correspondence and requests for materials should be addressed to J.A.S.K. (e-mail: kelso@walt.ccs.fau.edu). For data animation (MPEG format), see http://www.ccs.fau.edu.

Lipids are required for directional pollen-tube growth

Mieke Wolters-Arts, W. Mary Lush* & Celestina Mariani

Graduate School Experimental Plant Sciences, Department of Experimental Botany, University of Nijmegen, Toernooiveld 1, 6525 ED Nijmegen, The Netherlands

* *Plant Cell Biology Research Centre, School of Botany, University of Melbourne, Parkville, Victoria 3052, Australia*

Successful pollination and fertilization are absolute requirements for sexual reproduction in higher plants. Pollen hydration, germination and penetration of the stigma by pollen tubes are influenced by the exudate on wet stigmas[1] and by the pollen coat in species with dry stigmas[2–5]. The exudate allows pollen tubes to grow directly into the stigma, whereas the pollen coat establishes the contact with the stigma. Pollen tubes then grow into the papillae, which are covered by a cuticle. The components of the exudate or pollen coat that are responsible for pollen tube penetration are not known. To discover the role of the exudate, we tested selected compounds for their ability to act as functional substitutes for exudate in the initial stages of pollen-tube growth on transgenic stigmaless tobacco plants[1] that did not produce exudate. Here we show that lipids are the essential factor needed for pollen tubes to penetrate the stigma, and that, in the presence of these lipids, pollen tubes will also penetrate leaves. We propose that lipids direct pollen-tube growth by controlling the flow of water to pollen in species with dry and wet stigmas.

In transgenic, female-sterile tobacco plants in which the secretory zone of the stigma is ablated by expression of the cytotoxic gene *STIG 1-barnase*, pollen tubes only penetrate the stigma and successfully fertilize ovules when stigma exudate of wild-type plants is applied to the ablated stigmas[1,6]. To determine whether stigma function is also restored by exudates of other plant species, we applied the lipid-rich[7] exudate of *Petunia* (a close relative of tobacco), and the carbohydrate-rich[8] exudate of lily (a distantly related species) to the stigmas. With *Petunia* exudate, pollen tube penetration and seed setting occurred (Fig. 1a). Application of lily exudate resulted in pollen hydration and germination, but not penetration (Fig. 1b), indicating that lipids in the exudate may play a role in pollen tube penetration.

The lipid fraction of the exudate contains many saturated and unsaturated fatty acids, which usually occur as triacylglycerides[9,10]. To determine whether triacylglycerides are involved in pollen tube penetration, we applied a purified oil with a fatty-acid composition similar to that of exudate to stigmaless pistils. Application of this oil restored stigma function and resulted in seed production. Addition of the same oil in a 1:1 mixture of oil and lily exudate also restored the ability of pollen tubes to penetrate the stigma (see Methods). To investigate the effect of individual components of the purified oil, we applied the unsaturated triacylglycerides triolein, trilinolein and trilinolenin. Only application of trilinolein allowed penetration of enough pollen tubes into the style (Fig. 1c) to result in seed production. In contrast, a liquid mixture of saturated triacylglycerides did not result in pollen tube penetration (Fig. 1d; see Methods).

We investigated the effects of the products of breakdown of triacylglycerides by applying glycerol, free fatty acids (oleic, linoleic or linolenic acid), monolinolein or dilinolein. None of these products allowed penetration of enough pollen tubes into the style (see Methods). In the presence of trilinolelaidin, the *trans* form of trilinolein, pollen tubes penetrated the stylar tissue, but were immediately arrested and exhibited severe deformations. Oils that are not based on triacylglycerides, such as silicon oils, did not restore stigma function (see Methods). These data indicate that *cis*-unsaturated triacylglycerides are sufficient and essential for the normal functioning of the exudate.

In genera with dry stigmas, such as *Brassica* and *Arabidopsis*, the

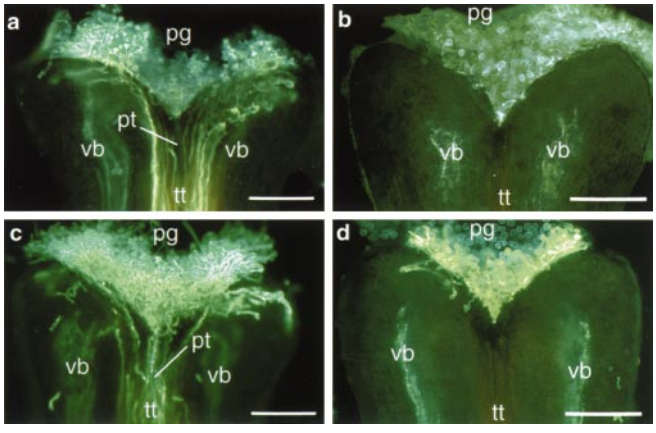

Figure 1 Fluorescence micrographs of longitudinal sections of stigmaless pistils 24 h after pollination. **a,** After application of *Petunia* exudate, pollen grains on the stigmaless surface become hydrated and germinate and the pollen tubes penetrate the stylar tissue. The effects of application of **b,** *Lilium* exudate, **c,** trilinolein, and **d,** saturated triacylglycerides are also shown (see Methods). Bars represent 100 μm. Abbreviations are as follows: pg, pollen grain; pt, pollen tube; tt, transmitting tissue; vb, vascular bundle.